JURNAL SAINS MATERI INDONESIA (JUSAMI)
ISSN: 1411-1098 (print), 2614-087X (online)
VOL. 25, ISSUE 2, 2024
DOI:10.55981/jsmi.2024.3134

ORIGINAL ARTICLE

Carbon Nanotube Modified Poly HEMA/CNC Composite Sorbent for Selective Recovery of Rare Earth Metal Ions

N. Jamilah[1,2], A. Riswoko[2] and A. B. Cahaya *[1]

[1]Department of Physics, Faculty of Mathematics and Natural Sciences, Universitas Indonesia, Indonesia
[2]Research Center for Polymer Technology, National Research and Innovation Agency (BRIN), Indonesia

ABSTRACT – Rare earth elements (REEs) from secondary resources must be purified before being used as critical raw materials. A novel type of carbon nanotube (CNT)-based composite sorbents have been developed to adsorb REE metal ions from a low concentration of the aqueous solution. The composite sorbents prepared from 2-Hydroxyethyl methacrylate (HEMA), cellulose nanocrystal (CNC), and CNT were characterized by Fourier transform infrared (FTIR) and their adsorption properties by inductively coupled plasma-optical emission spectrometry (ICP-OES). The results showed that the adsorption performance of sorbents depends on their constituting materials and the pH of the feeding solution. The presence of CNTs in the sorbents helps increase adsorption efficiency while increasing contact time. The highest adsorption efficiency (98%) is achieved at pH 4 with a contact time of 90 minutes. The prepared composite sorbents show better adsorption selectivity for cerium (Ce^{3+}) ions than neodymium (Nd^{3+}) and lanthanum (La^{3+}).

ARTICLE HISTORY
Received: 15 Jan 2024
Revised: 01 Apr 2024
Accepted: 08 Apr 2024

KEYWORDS
Adsorption
Liquid crystal
Cellulose nanocrystal
Carbon nanotube
Rare earth element

INTRODUCTION

Rare earth elements (REEs) include 17 elements in the lanthanide group, which are classified into light REEs (LREEs, Sc, and La-Eu) and heavy REEs (HREEs, Y, and Gd -Lu) [1]. These materials are currently a trend in the development of renewable energy and environmentally friendly enterprises, especially for energy storage (electric batteries), energy conversion (solar cells, wind turbines, etc.), electric vehicles, and other electronics industries [2]–[4]. Because of the increased demand for REEs, many separation/preconcentration techniques, including ion exchange, precipitation, liquid-liquid extraction (LLE), and solid-phase extraction (SPE), have been applied [5]–[7]. Although LLE is more widely used on an industrial scale, its efficiency has always been questioned due to the inability to extract polar compounds, the tendency to form emulsions, the presence of impurities in the final product, the loss of extractants into the liquid phase, the long time required, the low product purity, and the removal of toxins or flammable chemicals [7]. Because of this, an innovative and effective separation method is needed for the extraction of REEs, one of which is a selective adsorption method using nanomaterials composite-based adsorbents in SPE.

Nanomaterials offer several advantages, such as high specific surface area, multifunctionality, amenability to further surface modification, and having many functional groups on their surface that facilitate interactions with species [8]. Thanks to these advantages, extraction efficiency, selectivity, quality, and contact area are expected to be improved, thereby reducing the consumption of chemicals in the separation and extraction of REEs. To use this method, the kinetics and adsorption capacity of the process will determine how efficiently the REEs are recovered [9]. Therefore, various types of nanomaterials have been developed, one of which is carbon nanotubes (CNTs) [9]–[11].

CNTs are a type of carbon-based materials having a diameter of a nanometer and a length of a micrometer (with a length-to-diameter ratio greater than 1,000), which are distinctive nanostructures with exceptional electrical and mechanical capabilities because of their close resemblance to graphene or their one-dimensional appearance [12]. Some researchers discovered that carbon nanotubes were more desirable than activated carbon and clay due to their great selectivity and advantageous physicochemical stability. In addition, carbon nanotubes have unique properties, i.e., excellent electrical characteristics, a sizable specific surface area, good superior thermal conductivity (2000–6000 W/m.K), a high elastic modulus (1000–3000 GPa), and a high tensile strength (50–100 GPa) [13], [14]. Therefore, CNTs have promising properties that can be utilized as the main component of the solid phase for REE recovery.

CNTs are commercially accessible in two forms: single-walled (SWCNTs) or multi-walled (MWCNTs), yet both lack inherent orientation. To enhance their properties, extensive research has been dedicated to developing methods for orienting these nanotubes, aiming to achieve superior-quality materials. One such method involves inducing order through liquid crystals (LCs), leveraging the orientation order of CNTs within LC matrices. [15], [16]. The transition of CNTs in liquid crystals is a thermodynamic phenomenon that occurs naturally when nanotubes are uniformly dispersed in a liquid medium at a sufficiently high concentration, leading to the formation of a nematic liquid crystal particle phase [15], [17]. Hence, to achieve a high degree of CNT orientation, the CNT is dispersed within a liquid crystal polymer (LCP), creating an inclusion structure within the liquid crystal phase, typically nematic and/or cholesteric. One

***CORRESPONDING AUTHOR** | A. B. Cahaya | adam@sci.ui.ac.id

commonly utilized liquid crystal polymer is cellulose nanocrystals (CNCs), which, when hybridized with SWCNT at specific concentrations, facilitates enhanced alignment (SWCNT/CNC)[18].

CNCs are predominantly derived from naturally occurring cellulose fibers. Their renewable and biodegradable nature renders them a sustainable and eco-friendly material suitable for various applications [19]–[21]. While these nanocrystals are predominantly hydrophilic, they can be surface-functionalized to meet diverse requirements, such as fabricating high-performance nanocomposites. This is achieved through the synthesis of crosslinked polymer networks via radical polymerization. [19].

To investigate the impact of sorbent formulation on the adsorption selectivity of REEs, such as lanthanum (La^{3+}), cerium (Ce^{3+}), and neodymium (Nd^{3+}), three types of hybrid adsorbents (designated I-III) were developed. These hybrid adsorbents were prepared to utilize different approaches: (**I**) SWCNT/CNC grafted with polyhydroxy ethyl methacrylate [p(HEMA-CNT/CNC)], (**II**) CNC grafted with polyhydroxy ethyl methacrylate [p(HEMA-CNC)], and (III) CNT blended with polyhydroxy ethyl methacrylate [p(HEMA-CNT)]. The kinetics and adsorption capacity of La^{3+}, Ce^{3+}, and Nd^{3+} will be assessed using standard mixed aqueous solutions.

EXPERIMENTAL METHOD

Materials and Instruments

Cellulose nanocrystals (CNCs) were purchased from CelluForce, Canada. 2-Hydroxyethyl methacrylate (HEMA), single-walled carbon nanotube (SWCNT), rare earth elements mix solution for inductively coupled plasma (ICP), N, N'-methylene bis acrylamide (MBA) as cross-linker, and Irgacure 2959 as a photo-initiator of polymerization (PI) were purchased from Sigma-Aldrich Co., Ltd, Germany. No additional purification was performed on any of the reagent components. The entire trial was conducted with distilled water.

The equipment used in this research, i.e., ultraviolet (UV) curing oven, Fourier transform infrared (FTIR), and inductively coupled plasma-optical emission spectrometry (ICP-OES). Ultraviolet (UV) curing oven from PT. AGTM Indonesia (Model no. AG-200-2PM) for radical polymerization of sample, Fourier transform infrared (FTIR) Bruker Sensor 27 for analyze the adsorbent's functional groups, inductively coupled plasma-optical emission spectrometry (ICP-OES) thermos-scientific iCAP 6000 series for analyze the residual La^{3+}, Ce^{3+}, and Nd^{3+} concentrations.

Method and Procedure

The SWCNT/CNC grafted with polyhydroxy ethyl methacrylate or [p(HEMA-CNT/CNC)] (**I**) adsorbent was prepared by mixing the component materials (CNT, HEMA, MBA, CNC, and irgacure 2959), followed by radical polymerization synthesis. In this experiment, the LC phase particle suspension was obtained by diluting the CNC solution containing 6 wt% CNC to 3 wt% CNC. Then, LC-CNC suspension was added into a mixture of CNT, HEMA, 4 wt% of Irgacure 2959, and MBA (0.1 g in 5 ml of H_2O) [18], [19], [22]. The ratio of CNT, CNC, and HEMA was 1:5:5. The process of mixing these component materials used horn ultrasonics at 12 W/ml for 40 minutes in an ice water bath to prevent temperature increases [22]. Next, the mixture was left for 24 hours, and then UV (ultraviolet) photopolymerization was carried out for 40 minutes at room temperature. With the same procedure, hybrid adsorbents (p(HEMA-CNC) (**II**) and p(HEMA-CNT) (**III**) were synthesized by reducing unnecessary components.

All prepared sorbents were characterized by Fourier transform infrared (FTIR) spectroscopy using KBr pellets to assess whether any reactions occurred during the mixing process by analyzing the functional groups present in the samples. Finally, the samples would be used in the adsorption experiment for evaluation of the selective adsorption of La^{3+}, Ce^{3+}, and Nd^{3+} ions.

Adsorption experiments were conducted using a batch method at ambient temperature (25°C). A 100 mg sample of adsorbent was immersed in 20 mL of a multi-element solution with an initial rare earth elements (REEs) mix concentration of 0.5 mg/L. The contact time varied (30, 60, 90, and 120 minutes) at pH 3.0 to examine the efficiency of adsorption by comparing the performance of the p(HEMA-CNT/CNC) (**I**), adsorbent with that of p(HEMA-CNC) (**II**), and p(HEMA-CNT) (**III**). Subsequently, the adsorption kinetics of p(HEMA-CNT/CNC) were investigated. The initial pH levels of REE ions solutions varied between 3, 4, and 6 which were modified to the appropriate values by dropwise of 3%v/v HNO_3 or 1 M of NaOH solutions. Initial concentrations of REEs mix solution ranging from 0.5 mg/L to 6 mg/L were used to study the adsorption isotherms. After the adsorption was processed, the adsorbents were separated from the solution by filtration with Sartorius 390 and a Whatman syringe filter. Then, ICP-OES was used to measure the residual La^{3+}, Ce^{3+}, and Nd^{3+} concentrations. The adsorption capacity or amount of REEs ion adsorbed (q_e) for this experiment was measured using Equation (1) [8], [23]:

$$q_e = \frac{(C_0 - C_e)\,V}{M} \tag{1}$$

where C_0 is the REEs concentration at the start of the experiment (mg/L), C_e is the REEs concentration at equilibrium (mg/L) in the aqueous solution, V is the total volume of the aqueous solution (mL), and M is the mass of the adsorbent (mg).

RESULT AND DISCUSSION

Figure 1 demonstrated Fourier transform infrared (FTIR) spectra for adsorbents of SWCNT/CNC grafted with polyhydroxy ethyl methacrylate or p(HEMA-CNT/CNC) (**I**), p(HEMA-CNC) (**II**), and p(HEMA-CNT) (**III**). Furthermore, the peaks were identified by the functional group analysis shown in Table 1. FTIR spectral data were used to analyze the surface functional groups present in p(HEMA-CNT/CNC) (**I**) by comparing with adsorbents of p(HEMA-CNC) (**II**) and p(HEMA-CNT) (**III**) to evaluate the mixing reaction occurs between carbon nanotube (CNT) and cellulose nanocrystals (CNC) with HEMA to increase the hydrophobicity of polymer or introduce reactive sites [19]. Apart from that, to determine ultraviolet (UV) photopolymerization occurs with the addition of Irgacure 2959 as a photo-initiator of polymerization (PI) and N, N'-methylene bis acrylamide (MBA) as a crosslinker. It is frequently possible to explore four zones with various bond types using the FTIR spectra: single bond (range 4000–2500 cm^{-1}), triple bond (range 2500–2000 cm^{-1}), double bond (range 2000–1500 cm^{-1}), and fingerprint region (< 1500 cm^{-1}) [24].

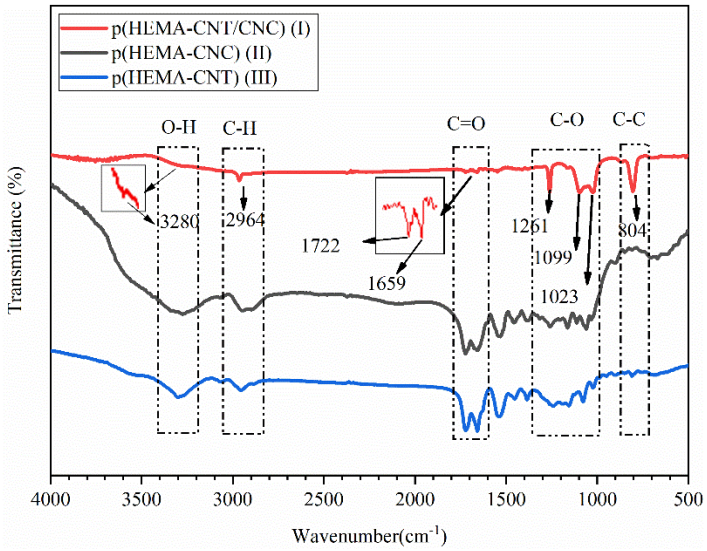

Figure 1. FTIR spectra of (**I**) p(HEMA-CNT/CNC), (**II**) p(HEMA-CNC), and (**III**) p(HEMA-CNT) adsorbents

Table 1. Identification of FTIR spectra for (**I**) p(HEMA-CNT/CNC) adsorbents

Peak Frequency (cm^{-1})	Functional Groups
3280	O-H
2964	C-H
1722	C=O (acrylate)
1659	C=O (amide)
1261	C-O (ester glucoside)
1099	C-O (ester glucoside)
1023	C-O (ester glucoside)
804	C-C

The FTIR observed the presence of peaks frequency around 3280, 2964, 1722-1659, 1261–1023, and 804 cm^{-1} as a result of the stretching vibration of O-H, C-H, C=O, C-O, and C-C groups, respectively [24],[25],[26]. The presence of peaks at 3280 cm^{-1} indicates O-H groups from cellulose nanocrystal (CNC) and 2-hydroxyethyl methacrylate (HEMA). The presence of C-H groups at 2964 cm^{-1} indicates stretching alkanes from CNC and HEMA. The presence of C=O in a peak of 1722 cm-1 indicates acrylate, which is a carboxyl group from HEMA. Indication of the presence of C-H and C=O shows that the addition of 3 wt% of HEMA succeeded in creating reactive sites with CNC and CNT. The presence of C=O also in the peak of 1659 cm-1 indicates amide, which is the carbonyl group from MBA. The peak existence of MBA indicates success in the polymerization process. Meanwhile, the C-O group in range peaks of 1261–1023 cm^{-1} indicates ester glucoside and the C-C group at 804 cm^{-1}, which are fingerprint regions of CNC and CNT, respectively. These results prove that the mixing reaction and UV photopolymerization of **(I)** p(HEMA-CNT/CNC) is successful (Figure 2).

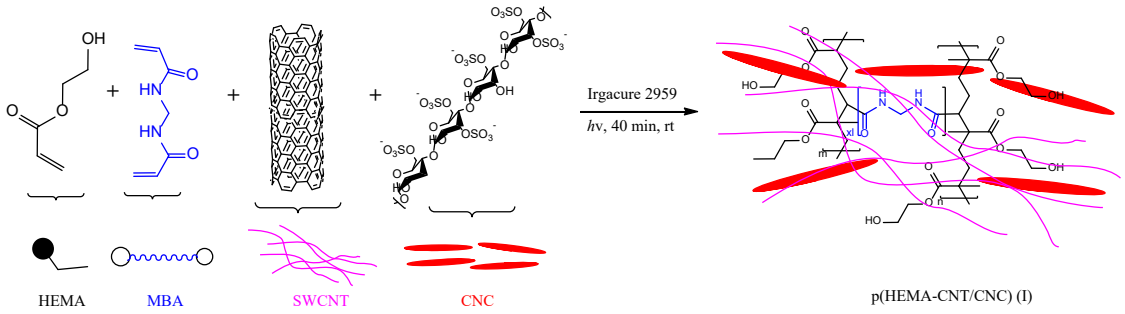

Figure 2. The mixing reaction and UV photopolymerization of **(I)** p(HEMA-CNT/CNC)

In order to study the effect of modifying CNTs into (**I**) p(HEMA-CNT/CNC) adsorbent on the selectivity of REE ions, a comparison of the adsorption efficiency (η), which is calculated on Equation (2) [23] for (**I**) p(HEMA-CNT/CNC), (**II**) p(HEMA-CNC), and (**III**) p(HEMA-CNT) adsorbents onto the contact time was presented in Figure 3.

$$\eta = \left(\frac{C_0 - C_e}{C_0}\right) X\ 100\% \qquad (2)$$

where C_0 is the REEs concentration at the start of the experiment (mg/L), and C_e is the REEs concentration at equilibrium (mg/L) in the aqueous solution.

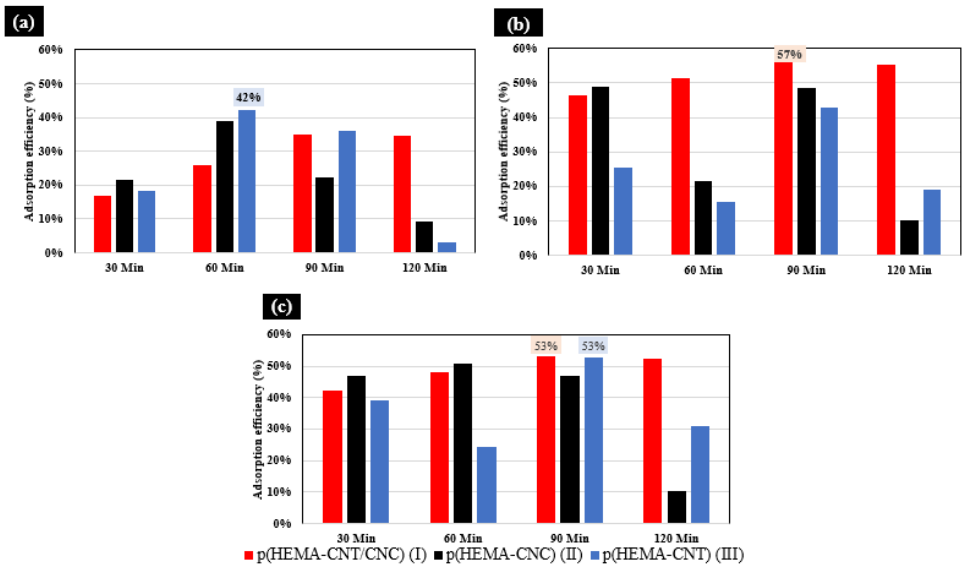

Figure 3. Adsorption efficiency of adsorbents in varied contact times (30, 60, 90, and 120 minutes) and ion REEs (a) La^{3+}; (b) Ce^{3+}; (c) Nd^{3+}

In Figure 3, the adsorbents (**I**) p(HEMA-CNT/CNC) and (**III**) p(HEMA-CNT), both incorporating CNTs, demonstrated remarkable adsorption efficiencies of rare earth element (REE) ions, reaching peaks of 42% for La^{3+}, 57% for Ce^{3+}, and 53% for Nd^{3+} ions. The adsorption capacity of this adsorbent was significantly affected by its surface area. As the size of the adsorbent decreases, its surface area increases, thereby enhancing the potential for chemical adherence and consequent adsorption [27]. From the BET (Brunauer Emmett Teller) test results, the surface area from the highest to the lowest is (**I**) p(HEMA-CNT/CNC); (**III**) p(HEMA-CNT), (**II**) and p(HEMA-CNC) with a value of 19.09 m^2/g; 16.65 m^2/g, and 11.27 m^2/g, respectively (Table 2). These results prove that the order of adsorption ability as the surface area increases are (**I**) p(HEMA-CNT/CNC) > (**III**) p(HEMA-CNT) > (**II**) p(HEMA-CNC). Apart from that, the selectivity of La^{3+} was more suitable for using (**III**) p(HEMA-CNT), Ce^{3+} using (**I**) p(HEMA-CNT/CNC), and Nd^{3+} using both (**I**) p(HEMA-CNT/CNC) and (**III**) p(HEMA-CNT).

Table 2. BET test results on hybrid adsorbent (**I**) p(HEMA-CNT/CNC), (**II**) p(HEMA-CNC), and (**III**) p(HEMA-CNT)

Adsorbent Type	Pore Radius (Å)	Pore Volume	Surface Area

		(× 10^{-2} cc/g)	(m^2/g)
(**I**) p(HEMA-CNT/CNC)	70.28	4.871	19.09
(**II**) p (HEMA- CNC)	31.44	3.274	11.27
(**III**) p(HEMA-CNT)	63.10	4.501	16.65

Another factor that influences the adsorption of adsorbents is surface charge [27]. In general, single-walled carbon nanotubes (SWCNTs) tend to have a neutral or slightly negative surface charge, particularly in their native form [28]. With modifications to CNTs, both (**I**) p(HEMA-CNT/CNC) and (**III**) p(HEMA-CNT) exhibit a more negatively charged nanocarbon surface compared to (**II**) p(HEMA-CNC) (II). This increased negativity arises from carbon oxidation, rendering the former two more hydrophilic and enriched with oxygen functional groups, including -O-H, C-H, C=O, and C-O groups, as indicated by the FTIR results discussed previously. These additional functional groups enable the formation of hydrogen bonds and Van der Waals interactions, thereby enhancing the adsorption capacity of the materials. Meanwhile, REE adsorption is controlled by electrostatic forces associated with various functional groups (O donor) and more positively charged [9],[29]. Therefore, the presence of this negative surface charge is able to increase the ion exchange ability of carbon materials and REE ions. This proves that the CNT modification in the adsorbent has the ability to adsorb REEs better than other adsorbent.

In addition, Figure 3 shows that the adsorption ability of (**I**) p(HEMA-CNT/CNC) tends to be stable after a contact time (equilibrium time) of 90 minutes compared to the others. This phenomenon may be attributed to the stable homogeneous dispersion of CNCs and CNTs, resulting in their alignment to form a nematic liquid crystal particle phase. The presence of this stable, uniformly dispersed surface enables numerous functional groups to serve as bonding sites for REE ions. Based on the literature, it provided profound abilities to increase the adsorption capacity and selectivity of REE ions [30]. These results provide that the modification of the CNT adsorbent in the form of (**I**) p(HEMA-CNT/CNC) is able to increase the adsorption capacity, efficiency, stability, and selectivity of Ce^{3+} compared to La^{3+} and Nd^{3+}. For the next step, it is necessary to study and optimize mixing/sonication time in the adsorbent preparation process to ensure the CNTs are perfectly oriented and homogeneously dispersed.

The two-step adsorption kinetic process is interpreted to the pseudo-first-order and pseudo-second-order models. Pseudo-first-order presumes that the adsorbate has been transferred from the bulk solution containing ion REEs to the adsorbent's surface. Pseudo-second-order presumes that the adsorbate is diffused and arranged inside the sorbent pores. For these models, the adsorption process with a rate-limiting step explains the adsorption mechanism [31]. Pseudo-first-order and pseudo-second-order models based on Equation (3) and (4), respectively [31]. In order to study the adsorption kinetics of La^{3+}, Ce^{3+}, and Nd^{3+} ions using (**I**) p(HEMA-CNT/CNC) adsorbents, the results of residual concentration which using ICP-OES (inductively coupled plasma-optical emission spectrometry) test has fitted to the pseudo-first-order and pseudo-second-order models (Figure 4) with kinetic constant in Table 3.

$$\ln(q_e - q_t) = \ln q_e - k_1 t \tag{3}$$

$$\frac{t}{q_t} = \frac{1}{k_2 q_e^2} + \frac{t}{q_e} \tag{4}$$

where k_1 (min^{-1}) is the rate constant for first-order adsorption, k_2 (g/mg·min^{-1}) is the rate constant for second-order adsorption, q_e (mg /g) is the adsorption capacity at equilibrium, and q_t (mg/g) is the adsorption capacity at any time t.

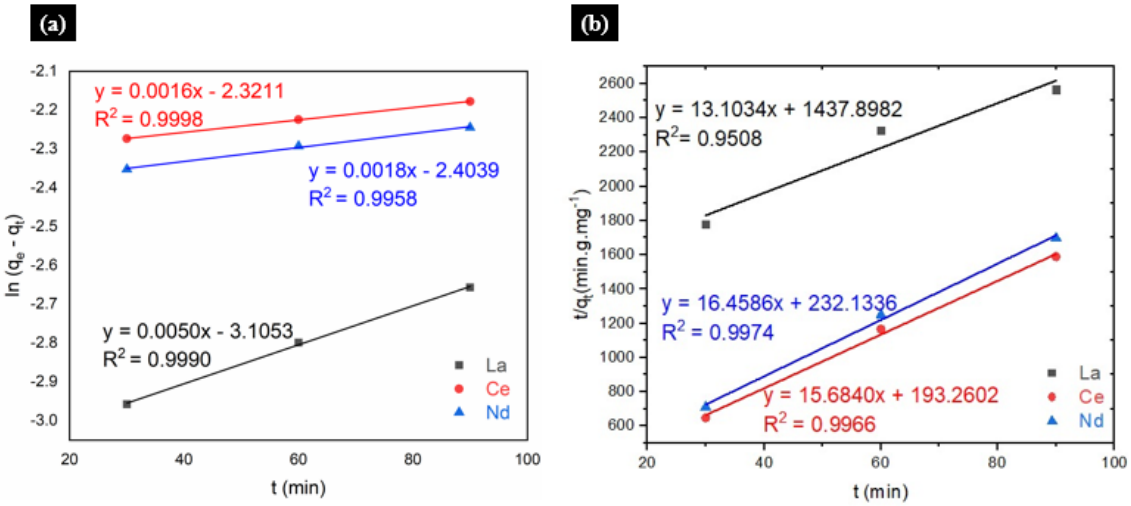

Figure 4. The adsorption kinetics of La^{3+}, Ce^{3+}, and Nd^{3+} ions using (**I**) p(HEMA-CNT/CNC) adsorbents has fitted to two models: (a) Pseudo-first-order and (b) Pseudo-second-order

Table 3. Parameters of pseudo-first-order and pseudo-second-order models for the adsorption kinetics of La^{3+}, Ce^{3+}, and Nd^{3+} ions using (**I**) p(HEMA-CNT/CNC) adsorbents

Kinetic Models	Parameters	La^{3+}	Ce^{3+}	Nd^{3+}
Pseudo-first-order	k_1 (min^{-1})	0.0050	0.0016	0.0018
	R^2	0.9990	0.9998	0.9958
Pseudo-second-order	k_2 (min^{-1})	0.1194	1.2728	1.1669
	R^2	0.9508	0.9966	0.9974

Based on Table 3, the interpretation of the adsorption mechanism that occurs in the adsorption of La^{3+}, Ce^{3+}, and Nd^{3+} ions using (**I**) p(HEMA-CNT/CNC) adsorbents can be studied. In the first stage, these third elements from the solution have been successfully transferred and attached to the surface of the adsorbent, forming a layer. This was proven by the value of the pseudo-first-order linear correlation coefficient (R^2), which is close to 1.00 and has almost the same adsorption rate constant (k_1) for all elements. At this stage, there is no change in the chemical structure due to the physical adsorption mechanism that takes place between the adsorbent and adsorbate. Next, in the second stage, there was diffusion and arrangement of metal ions into the pores of the adsorbent. The diffusion process of Ce^{3+} and Nd^{3+} ions is better than La^{3+} ion, which is indicated by the pseudo-second-order linear correlation coefficient (R^2) values of Ce^{3+} and Nd^{3+} ions approaching 1.00 (0.9966 and 0.9974), higher than La^{3+} (0.9508) with the adsorption rate constant (k_2) of La^{3+} ion, lower than Ce^{3+} and Nd^{3+} ions. At this stage, the mechanism of the type of adsorption that occurs between the adsorbate and the adsorbent, i.e., chemical adsorption, forms chemical bonds, and monolayer, which is more stable than the previous stage (pseudo-first-order). From these results, the (**I**) p(HEMA-CNT/CNC) adsorbent succeeded in adsorbing La^{3+}, Ce^{3+}, and Nd^{3+} ions and in forming a monolayer which the Ce^{3+} and Nd^{3+} monolayers more stable than the La^{3+} ion.

A crucial factor influencing the capacity of metal ions is the pH of the solution to adsorb to the (**I**) p(HEMA-CNT/CNC) adsorbent surface. Figure 5 demonstrates the adsorption efficiency values based on Equation (1) of La^{3+}, Ce^{3+}, and Nd^{3+} onto (**I**) p(HEMA-CNT/CNC) adsorbent with varied pH.

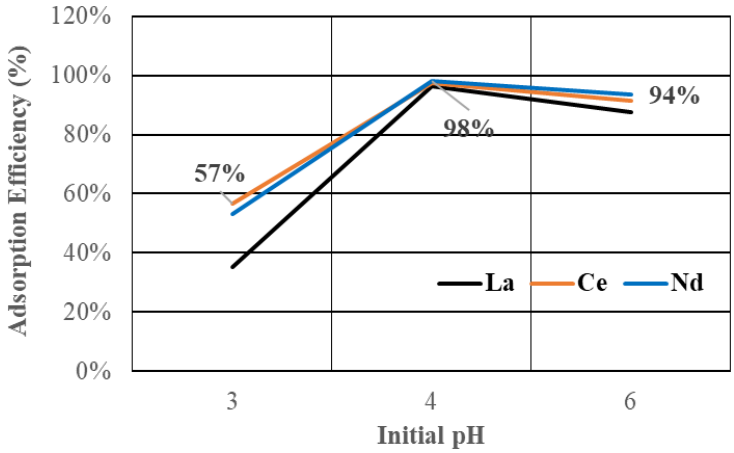

Figure 5. Effect of pH on the adsorption efficiency (%) of La^{3+}, Ce^{3+}, and Nd^{3+} onto (**I**) p(HEMA-CNT/CNC) adsorbent

As shown in Figure 5, increasing the initial pH of solution aligns with the adsorption efficiency with optimum pH, which provides the highest adsorption efficiency (± 98%) occurs at pH 4. This increase is due to the surface of the nanocarbon-based adsorbent experiencing deprotonation of the hydroxyl groups [8]. Therefore, the surface charge of the adsorbent is more negative, which facilitates ion exchange with the positively charged REEs. Meanwhile, at low pH, the adsorbent tends to aggregate. This aggregation is caused by repulsive forces between metal cations and the protonated and positively charged adsorbent surface [8], [32]. However, these results show the adsorption efficiency of La^{3+} increases significantly compared to Ce^{3+} and Nd^{3+} ions at pH > 3. Drawing from findings in other studies regarding La^{3+} adsorption, it has been emphasized that pH stands out as one of the pivotal process factors directly influencing La^{3+} adsorption by adsorbents. This is due to its ability to impact both the degree of La^{3+} ionization and the surface properties of the adsorbent. Notably, the optimal adsorption capacity is typically attained within the pH range of 4–6. Thus, the adsorbent is efficient enough to adsorb La^{3+} at pH 4 due to the presence of different functional groups and in the acidic region (i.e., pH 3) due to electrostatic repulsion between surface functional groups and H^+ ions. Meanwhile, at pH >6, the deposition of La3+ occurs due to the formation of $La(OH)_3$ because of hydrolysis at alkaline pH [33]. From these results, the initial pH of the solution is important to the selectivity of La^{3+}, Ce^{3+}, and Nd^{3+}. It can be concluded that the adsorption selectivity of La^{3+}, Ce^{3+}, and Nd^{3+} using p(HEMA-CNT/CNC) (**I**) adsorbent occurs at pH < 4 (i.e., pH 3) with a maximum adsorption efficiency of around 57%.

The interaction of a substrate containing La^{3+}, Ce^{3+}, and Nd^{3+} from the bulk solution with the surface of the (**I**) p(HEMA-CNT/CNC) adsorbent is described by the adsorption isotherms. It means a relationship between the concentration of the substrate in the bulk solution at a certain temperature and the amount of substrate adsorbed per unit mass of adsorbent [31]. In order to study the adsorption isotherm of La^{3+}, Ce^{3+}, and Nd^{3+} ions using (**I**) p(HEMA-CNT/CNC) adsorbent, the results of residual concentration which is determined by ICP-OES fitted to Langmuir and Freundlich models based on Equation (5) and (6), respectively (Figure 6). In addition, the adsorption factor of Langmuir models (R_L) using Equation (7) [23], [31].

$$\frac{C_e}{q_e} = \frac{1}{q_m K_L} + \frac{C_e}{q_m} \tag{5}$$

$$\log q_e = \log K_f + \frac{1}{n} \log C_e \tag{6}$$

$$R_L = \frac{1}{1 + K_L C_o} \tag{7}$$

where q_m is the maximum adsorption capacity (mg/L), K_L is a constant in Langmuir models, K_f is the Freundlich isotherm constant, and n is the adsorption intensity. The value of R_L indicates that the behavior of the isotherm is described as unfavorable adsorption ($R_L > 1$), linear adsorption ($R_L = 1$), no adsorption ($R_L = 0$), and favorable adsorption ($0 < R_L < 1$), where C_o is the highest initial concentration [23],[31].

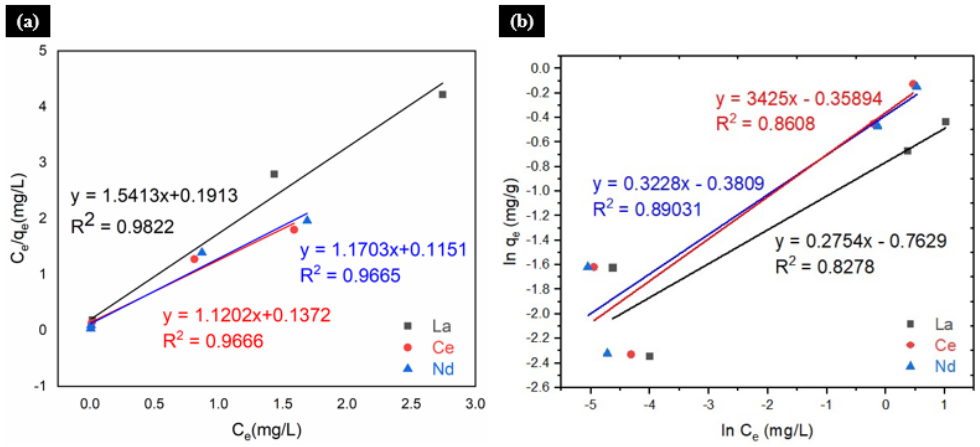

Figure 6. The adsorption isotherm of La^{3+}, Ce^{3+}, and Nd^{3+} using (I) p(HEMA-CNT/CNC) adsorbent has fitted to two models: (a) Langmuir, (b) Freundlich

As results in Figure 6, the Langmuir model matches the experimental data more well than the Freundlich model with a greater correlation coefficient (R^2) of 0.9822, 0.9666, and 0.9665 for the adsorption of La^{3+}, Ce^{3+}, and Nd^{3+} +, respectively. In addition, the behavior of the isotherm is indicated as favorable adsorption ($0 < R_L < 1$) with values of 0.0301, 0.0297, and 0.0240 for the adsorption of La^{3+}, Ce^{3+}, and Nd^{3+}, respectively. According to the results, REEs are adsorbed at particular sites on the surface of (**I**) p(HEMA-CNT/CNC) adsorbent and form a monolayer without any molecular attraction on the surface of the adsorbate. Because of that, this adsorbent is suitable for the adsorption of REE ions at low concentrations.

The maximum adsorption capacities (q_m) of La^{3+}, Ce^{3+}, and Nd^{3+} adsorption from the Langmuir model are 0.649, 0.893, and 0.854 mg/g, respectively. The maximum adsorption capacity of adsorbents is following their electronegativity and effective ionic radius. The order of electronegative values for these elements is $Nd^{3+} > Ce^{3+} > La^{3+}$, while the order of effective ionic radius values is the opposite of the order of electronegative values. In this experiment, the Ce^{3+} ion adsorption capacity is the highest but not significantly different from Nd^{3+}. This is possibly caused by Ce^{4+} ions in the aqueous solution, in which only this ion is stable while other REE ions are unstable [1], [34]. Ce is known for its unique redox behavior, which can exist in both trivalent (Ce^{3+}) and tetravalent (Ce^{4+}) oxidation states under ambient conditions. This redox flexibility allows cerium to participate in redox reactions during adsorption processes, which can enhance its adsorption capacity compared to Nd, which typically exists in the trivalent state [1], [34]. However, the results of their maximum adsorption capacities obtained are low because the concentration of ion REEs in the feeding solution is low, about 0.5–6 ppm with 100 mg of adsorbent. Generally, increasing the adsorbent dosage leads to higher adsorption capacity. This happened because more adsorbent material is available to capture the target molecules from the solution. In addition, higher feed concentrations resulted in higher adsorption capacities. This is because more adsorbate molecules are available in the solution for adsorption [27]. In order to increase adsorption capacities, it is important to optimize and study the effect of adsorbent dose and concentration of ion REEs in the feeding solution. According to the results, (**I**) p(HEMA-CNT/CNC) adsorbent is a good choice for the separation and selectivity of several types of REE^{3+} from aqueous solutions.

CONCLUSION

Studies have been done to determine how the SWCNT/CNC grafted with polyhydroxy ethyl methacrylate or (**I**) p(HEMA-CNT/CNC) adsorbent influences the adsorption selectivity of La^{3+}, Ce^{3+}, and Nd^{3+} ions. Experimental results show that the surface of (**I**) p(HEMA-CNT/CNC) adsorbent containing cellulose nanocrystal (CNC) in a hybrid liquid crystal phase with carbon nanotube (CNT) success in providing electrostatic interactions between rare earth element ions (REE^{3+}) and functional groups containing oxygen as of is able to adsorb La^{3+}, Ce^{3+}, and Nd^{3+} ions. This is proven by the high adsorption efficiency value of the (**I**) p(HEMA-CNT/CNC) adsorbent. The adsorption efficiency of this adsorbent is greatly influenced by the pH of the solution and the constituent materials. Due to the inclusion of CNTs in the adsorbent, the adsorption efficiency improves as contact time increases. The maximum adsorption efficiency (98%) is attained at pH 4 and 90 minutes of contact time. Additionally, the adsorption kinetics and isotherms are studied. The results of the kinetic analysis show that there are two stages of the adsorption process, i.e., the transfer process on the

surface/physical adsorption and then the penetration process into the surface pores of the adsorbent/chemical adsorption as of forming a monolayer. The sequence of maximum adsorption capacities (qm) derived from the Langmuir model closely aligns with those calculated manually (Equation (1)), showing $Ce^{3+} > Nd^{3+} > La^{3+}$ affinity on the (**I**) p(HEMA-CNT/CNC) adsorbent. Specifically, the values obtained via the nonlinear Langmuir model are 0.893 mg/g for Ce^{3+}, 0.854 mg/g for Nd^{3+}, and 0.649 mg/g for La^{3+}, respectively. Based on the obtained results, it is evident that the (**I**) p(HEMA-CNT/CNC) adsorbent emerges as a favorable option for effectively separating and selectively adsorbing various types of REE^{3+} from aqueous solutions. Notably, it demonstrates superior adsorption selectivity for cerium ions (Ce^{3+}) over neodymium (Nd^{3+}) and lanthanum (La^{3+}).

ACKNOWLEDGEMENT

The authors acknowledge the Research Center for Polymer Technology Laboratory, The National Research and Innovation Agency (BRIN). The authors acknowledge financial support from the Faculty of Mathematics and Natural Science, Universitas Indonesia, via FMIPA research grant 2023–2024.

REFERENCES

[1] J. H. L. Voncken. "Physical and chemical properties of the rare earths," in *The Rare Earth Elements: An Introduction*, Springer Briefs in Earth Sciences, 2016, pp. 53–72.
[2] A. R. Jha. *Rare Earth Materials: Properties and Applications*. CRC Press, 2014.
[3] M. Humphries. "Rare earth elements: The global supply chain." Congressional Research Service, 2010, pp. 1–20, 2011.
[4] V. Balaram. "Rare earth elements: A review of applications, occurrence, exploration, analysis, recycling, and environmental impact." *Geosci. Front.*, vol. 10, no. 4, pp. 1285–1303, 2019.
[5] H. Royen and U. Fortkamp. *Rare earth elements: Purification, sustainability and recycling*." IVL Svenska Miljöinstitutet, 2016.
[6] M. Kaya. "Recovery of metals and nonmetals from electronic waste by physical and chemical recycling processes." *Waste Manag.*, vol. 57, pp. 64–90, 2016.
[7] N. N. Hidayah and S. Z. Abidin. "The evolution of mineral processing in extraction of rare earth elements using solid-liquid extraction over liquid-liquid extraction: A review." *Miner. Eng.*, vol. 112, pp. 103–113, 2017.
[8] R. M. Ashour, H. N. Abdelhamid, A. F. Abdel-Magied, A. A. Abdel-Khalek, M. M. Ali, A. Uheida, M. Muhammed, X. Zou, and J. Dutta. "Rare earth ions adsorption onto graphene oxide nanosheets." *Solvent Extr. Ion Exch.*, vol. 35, no. 2, pp. 91–103, 2017.
[9] C. E. D. Cardoso, J. C. Almeida, C. B. Lopes, T. Trindade, C. Vale, and E. Pereira. "Recovery of rare earth elements by carbon-based nanomaterials—A review." *Nanomaterials*, vol. 9, no. 6, 2019.
[10] S. Tong, S. Zhao, W. Zhou, R. Li, and Q. Jia. "Modification of multi-walled carbon nanotubes with tannic acid for the adsorption of La, Tb and Lu ions." *Microchim. Acta*, vol. 174, pp. 257–264, 2011.
[11] D. L. Ramasamy, V. Puhakka, B. Doshi, S. Iftekhar, and M. Sillanpää. "Fabrication of carbon nanotubes reinforced silica composites with improved rare earth elements adsorption performance." *Chem. Eng. J.*, vol. 365, pp. 291–304, 2019.
[12] A. Aqel, K. M. M. A. El-Nour, R. A. A. Ammar, and A. Al-Warthan. "Carbon nanotubes, science and technology part (I) structure, synthesis and characterisation." *Arab. J. Chem.*, vol. 5, no. 1, pp. 1–23, 2012.
[13] M. Rajabi, K. Mahanpoor, and O. Moradi. "Removal of dye molecules from aqueous solution by carbon nanotubes and carbon nanotube functional groups: Critical review." *RSC Adv.*, vol. 7, pp. 47083–47090, 2017.
[14] S. Ho. "Low-cost adsorbents for the removal of phenol/phenolics, pesticides, and dyes from wastewater systems: A review." *Water (Switzerland)*, vol. 14, no. 20, 2022.
[15] N. Puech, C. Blanc, E. Grelet, C. Zamora-Ledezma, M. Maugey, C. Zakri, E. Anglaret, and P. Poulin. "Highly ordered carbon nanotube nematic liquid crystals." *J. Phys. Chem. C*, vol. 115, no. 8, pp. 3272–3278, 2011.
[16] C. Zakri. "Carbon nanotubes and liquid crystalline phases." *Liq. Cryst. Today*, vol. 16, no. 1, pp. 1–11, 2007.
[17] C. Zakri, C. Blanc, E. Grelet, C. Zamora-Ledezma, N. Puech, E. Anglaret, and P. Poulin. "Liquid crystals of carbon nanotubes and graphene." *Philos. Trans. R. Soc. A Math. Phys. Eng. Sci.*, vol. 371, no. 1988, p. 20120499, 2013.
[18] M. Jiang, R. Seney, P. C. Bayliss, and C. L. Kitchens. "Carbon nanotube and cellulose nanocrystal hybrid films." *Molecules*, vol. 24, no. 14, 2019.
[19] S. Hosseinzadeh, H. Hosseinzadeh, and S. Pashaei. "Fabrication of nanocellulose loaded poly(AA-*co*-HEMA) hydrogels for ceftriaxone controlled delivery and crystal violet adsorption." *Polym. Compos.*, vol. 40, no. S1, pp. E559–E569, 2019.
[20] G. R. Mahdavinia, H. Aghaie, H. Sheykhloie, M. T. Vardini, and H. Etemadi. "Synthesis of CarAlg/MMt nanocomposite hydrogels and adsorption of cationic crystal violet." *Carbohydr. Polym.*, vol. 98, no. 1, pp. 358–365, 2013.
[21] M. Constantin, I. Asmarandei, V. Harabagiu, L. Ghimici, P. Ascenzi, and G. Fundueanu. "Removal of anionic dyes from aqueous solutions by an ion-exchanger based on pullulan microspheres." *Carbohydr. Polym.*, vol. 91,

no. 1, pp. 74–84, 2013.
[22] D. Puspitasari, W. Budhijanto, E. Purnomo, and P. S. Nugraheni. "Optimization of Irgacure® 2959 Concentration as Photo-Initiator on Chitosan-Alginate Based Hydrogel for Colon Tissue Sealant." *Int. J. Technol.*, vol. 13, no. 8, pp. 1704–1714, 2022.
[23] A. B. D. Nandiyanto. "Isotherm adsorption of carbon microparticles prepared from pumpkin (Cucurbita maxima) seeds using two-parameter monolayer adsorption models and equations." *Moroccan J. Chem.*, vol. 8, no. 3, pp. 745–761, 2020.
[24] M. A. Mohamed, J. Jaafar, A. F. Ismail, M. H. D. Othman, and M. A. Rahman, "Chapter 1-Fourier Transform Infrared (FTIR) Spectroscopy." in *Membrane characterization*. N. Hilal, A. F. Ismail, T. Matsuura, and D. Oatley-Radcliffe, Eds. Elsevier, 2017, pp. 3–29.
[25] E. Vargün and A. Usanmaz. "Degradation of poly(2-hydroxyethyl methacrylate) obtained by radiation in aqueous solution." *J. Macromol. Sci. Part A Pure Appl. Chem.*, vol. 47, no. 9, pp. 882–891, 2010.
[26] J. P. De Mesquita, C. L. Donnici, I. F. Teixeira, and F. V. Pereira. "Bio-based nanocomposites obtained through covalent linkage between chitosan and cellulose nanocrystals." *Carbohydr. Polym.*, vol. 90, no. 1, pp. 210–217, 2012.
[27] N. Jamilah, A. B. Cahaya, and A. Riswoko. "Adsorption using selective adsorbents as an effective method for rare earth elements recovery – A review." *Reaktor*, vol. 23, no. 3, pp. 77–91, 2024.
[28] E. E. Christensen, M. Amin, T. M. Tumiel, and T. D. Krauss. "Localized charge on surfactant-wrapped single-walled carbon nanotubes." *J. Phys. Chem. Lett.*, vol. 13, no. 46, pp. 10705–10712, 2022.
[29] M. Badiei, N. Asim, M. Mohammad, M. Alghoul, N. A. Samsudin, M. Akhtaruzzaman, and N. Amin, K. Sopian. "Chapter 13-New graphene nanocomposites-based adsorbents." In *Handbook of Nanomaterials for Wastewater Treatment: Fundamentals and Scale Up Issues*. B. Bhanvase, S. Sonawane, V. Pawade, and A. Pandit, Eds. Elsevier, 2021, pp. 317–416.
[30] L. Zhao, X. Duan, M. R. Azhar, H. Sun, X. Fang, and S. Wang. "Selective adsorption of rare earth ions from aqueous solution on metal-organic framework HKUST-1." *Chem. Eng. J. Adv.*, vol. 1, p. 100009, 2020.
[31] M. Alaqarbeh. "Adsorption phenomena: Definition, mechanisms, and adsorption types: Short review." *RHAZES Green Appl. Chem.*, vol. 13, pp. 43–51, 2021.
[32] A. Y. Romanchuk, A. S. Slesarev, S. N. Kalmykov, D. V. Kosynkin, and J. M. Tour. "Graphene oxide for effective radionuclide removal." *Phys. Chem. Chem. Phys.*, vol. 15, no. 7, pp. 2321–2327, 2013.
[33] S. Iftekhar, D. L. Ramasamy, V. Srivastava, M. B. Asif, and M. Sillanpää. "Understanding the factors affecting the adsorption of Lanthanum using different adsorbents: A critical review." *Chemosphere*, vol. 204, pp. 413–430, 2018.
[34] D. A. Atwood. *The Rare Earth Elements: Fundamentals and Applications*. John Wiley & Sons Ltd, 2012, pp. 4–5, 2012.